applied sciences

MDPI

Article

Orthogonal Test on the True Triaxial Mechanical Properties of Frozen Calcareous Clay and Analysis of Influencing Factors

Chuan-Xin Rong [1], Zhi Wang [1,2,*], Yi Cao [1], Qing Yang [1] and Wei Long [1]

[1] School of Civil Engineering and Architecture, Anhui University of Science and Technology, Huainan 232001, China
[2] Anhui Provincial Key Laboratory of Building Structure and Underground, Anhui Jianzhu University, Hefei 230601, China
* Correspondence: wangz519714795@163.com

Abstract: In the Huainan and Huaibei mining areas, a layer of calcareous clay is buried deep in the surface soil layer (at approximately 400 m). This layer is in a high-stress state and is prone to freezing pipe fractures in the freezing method. To obtain the true triaxial mechanical properties of this clay in its frozen state, this study conducted a cross test ($L_{16}(4^5)$) to explore the change law of the strength of frozen calcareous clay under the influence of multiple factors. The results showed that the true triaxial stress–strain curve of frozen calcareous clay was divided into three stages: the strain within 0.5% showed linear elasticity. Under compressive stress, ice crystals and their cements were damaged or melted and shrank. At approximately 5%, they showed plastic hardening. The soil particles and ice crystals in the frozen soil recombined and became denser, resulting in irreversible deformation. As the compression progressed, cracks bred and swelled. The failure stage was manifested as strain hardening due to the test loading conditions. As the deformation increased, the stress also slightly increased. The consistent strength-influencing factors could be obtained through range and hierarchy analyses. The primary and secondary order of influence of σ_1 was the confining pressure σ_3, water content ω, temperature T, Bishop parameter b, and salt content ψ. The influence weight of each factor was quantitatively calculated. In the significance analysis, when the interaction was not considered, the effects of the pressure and moisture content on the strength were always significant. The effect of temperature was significant only when the significance level $\Omega > 0.05$. The salt content and b value had no significant influence on the strength, and the significance of each factor followed the order of the results of the range analysis method and analytic hierarchy process; when considering the interaction, the interaction factors had different effects on the strength. When $\Omega > 0.01$, the influence of factor A (temperature T) × B (water content ω) on the strength showed significance, even exceeding that of temperature. This demonstrated that when studying the strength characteristics of frozen soil, it is necessary to comprehensively consider the various factors and their interaction to more accurately characterize the mechanical behavior of frozen solids.

Keywords: frozen calcareous clay; true triaxial orthogonal test; analytic hierarchical process; significance test; interaction

check for updates

Citation: Rong, C.-X.; Wang, Z.; Cao, Y.; Yang, Q.; Long, W. Orthogonal Test on the True Triaxial Mechanical Properties of Frozen Calcareous Clay and Analysis of Influencing Factors. *Appl. Sci.* **2022**, *12*, 8712. https://doi.org/10.3390/app12178712

Academic Editors: Jie Zhou, Kai-Qi Li and Jun Hu

Received: 24 July 2022
Accepted: 26 August 2022
Published: 30 August 2022

Publisher's Note: MDPI stays neutral with regard to jurisdictional claims in published maps and institutional affiliations.

Copyright: © 2022 by the authors. Licensee MDPI, Basel, Switzerland. This article is an open access article distributed under the terms and conditions of the Creative Commons Attribution (CC BY) license (https://creativecommons.org/licenses/by/4.0/).

1. Introduction

The geotechnical strength index is an important survey parameter for the development and utilization of underground space. Under normal circumstances, conventional soil is considered a two- (saturated) or three-phase system, and laboratory testing and research have been conducted on such soils. For shallow rock and soil, the unconfined uniaxial compressive strength under different factors have been considered [1–3]. Such soils meet the engineering requirements; however, when the deep rock and soil are in a state of high stress, the contribution of the confining pressure to the strength cannot be ignored. To simulate a real stress environment, it was necessary to conduct false or true triaxial indoor

tests [4–6]. The factors influencing the strength in such tests include the water content (or saturation), soil properties, loading rate, confining pressure, and dry density. The strength of conventional soil is generally low, and the influence of various factors on the strength was not significant. Frozen soil is a four-phase system. Artificial ground freezing curtains are used as temporary support measures in major underground projects such as coal mine shaft excavation, subway tunnels, and special underground spaces. The influence of various factors on the properties of frozen structures, such as thermal conductivity [7,8] and strength, is greatly enhanced and more complex. Cai [9] conducted an unconfined compressive strength test on frozen clay under different water and Na_2SO_4 contents. The test results showed that the deformation of frozen soil was significantly affected by the change in the water and salt contents. Its strength increased to the maximum value first and then decreased with the increase of water content and salt content. Through a series of triaxial tests, Niu [10] found that the deformation and strength of frozen soil were significantly affected by temperature, moisture, and pressure. When the moisture content was low, and the confining pressure increased, a silty clay transitioned from strain softening to strain hardening. With the increase in the water content, the initial tangent modulus gradually changed from a linear distribution to a parabolic one with the confining pressure. Lai [11] and Du [12] analyzed the change characteristics of sand strength with the moisture content at different temperatures and the dependence of sand strength on the temperature under the same moisture content; the influence of moisture content on the strength of frozen soil did not purely depend on the moisture content. For a certain type of soil, there is a fixed moisture content (optimal moisture content). When it is greater than this value, the strength of frozen soil decreases with the increase in the moisture content [9,13–17]. The temperature, water content, salt content, and confining pressure significantly affect the strength of frozen soil. In terms of true triaxiality, the influence of Bishop parameter b on the strength of frozen soil, particularly the second principal stress, cannot be ignored. Hence, scholars have conducted true triaxial tests that are more representative of the real stratum stress state. For example, Dai [18] discussed the effects of the water content, consolidated confining pressure, and intermediate principal stress ratio on the strength of branched clay and reached a reliable conclusion. As reported by Chen [19], when the consolidated confining pressure was less than the structural strength of the structural loess, the stress–strain curve was a softening type; otherwise, it was a hardening type. Ma [20] and Zhang [21] conducted a true triaxial test on frozen sand under the influence of Bishop parameter b and accordingly performed an analysis.

Many factors affect the strength of frozen soil, not just the ones mentioned in the above studies. Most scholars considered only two or three of the many factors, and research on the interaction effects of the various factors is lacking. Hence, in this study, we considered a layer of calcareous clay in the deep surface of the Huainan and Huaibei mining area (buried at approximately 400 m) as the research object. This layer is in a high-stress state and highly prone to freezing pipe fractures in the freezing method. To obtain the true triaxial mechanical properties of this clay in its frozen state, we conducted true triaxial orthogonal tests on calcareous clay under the influence of five factors: temperature, water content, salt content, confining pressure, and Bishop parameter b. The primary and secondary order of influence of the various factors on the strength of the frozen soil was analyzed, and the weight of the influence of each factor on the peak strength was quantitatively calculated through the analytic hierarchy process. Finally, the interaction and non-interaction between the factors were considered, and statistical theory was applied to elaborate the influence of each factor. The degree of significance provided a certain reference value for the design and construction of underground structures in frozen soil.

2. Test Design and Test Results

2.1. Orthogonal Experimental Design Scheme

Frozen soil is used as a curtain for coal mine shaft excavation, and its strength is an important design index. Studies have shown that many factors affect the strength of frozen

soil, including water and salt content, confining pressure, temperature, and indoor test loading rate. In this study, we used a calcareous clay exhibiting strong plasticity as the test object. Table 1 presents the basic physical properties of this clay. Considering the temperature, water and salt content, confining pressure, and intermediate principal stress coefficient b, a true triaxial test was conducted on the frozen calcareous clay. Because of the many factors considered and the large number of tests required, an orthogonal test method was used to explore the influence of the various factors on the strength of this frozen soil. The orthogonal test design is presented in Table 2. A five-factor four-level ($L_{16}(4^5)$) orthogonal test was conducted. The corresponding levels of each factor were: (Factor A) Temperature T = −5–−20 °C; (Factor B) water content ω = 15–22.5%; (Factor C) salt content ψ = 0–3%; (factor D) confining pressure σ_3 = 1–4 MPa; (Factor E) principal stress coefficient b = 0, 0.33, 0.67, and 1.

Table 1. Geotechnical test results of the studied frozen soil [22].

Soil Type	Moisture Content ω (%)	Wet Density ρ (g/cm^3)	Dry Density ρ_d (g/cm^3)	Specific Gravity G_s	Void Ratio	Liquid Limit ω_L (%)	Plastic Limit ω_P (%)	Plasticity Index I_P	Liquid Limit Index I_L
Calcium Clay	22.62	2.04	1.66	2.736	0.64	54	35	19	−0.65

Table 2. True triaxial test factors of calcareous clay and their corresponding levels. (Note: The salt content in this table was the salt content in 100 mL of pure water, that is, the mass percentage of anhydrous $CaCl_2$ [23]).

Five Factors \ Four Levels	L1	L2	L3	L4
Temperature T/°C (Factor A)	−5	−10	−15	−20
Moisture content ω/% (Factor B)	15	17.5	20	22.5
Salt content ψ/% (Factor C)	0.0	1.0	2.0	3.0
Confining pressure σ_3 /MPa (Factor D)	1	2	3	4
Bishop parameter b (Factor E)	0	0.33	0.67	1

2.2. Test Loading Mode

Sample preparation: The dimensions of the test block sample were 100 mm × 100 mm × 100 mm. After the undisturbed soil sample was dried, ground, and sieved, it was sprayed with different concentrations of $CaCl_2$ solution in layers, mixed evenly, placed in a Ziplock bag, and allowed to stand for 24 h. The sample was then controlled using the dry density and volume. The mixed soil samples of corresponding quality were packed in a grinding tool in layers and pressed to prepare standard samples for use, as shown in Figure 1. Before the test, the standard sample was frozen at the required low temperature for more than 48 h, and a true triaxial test was conducted.

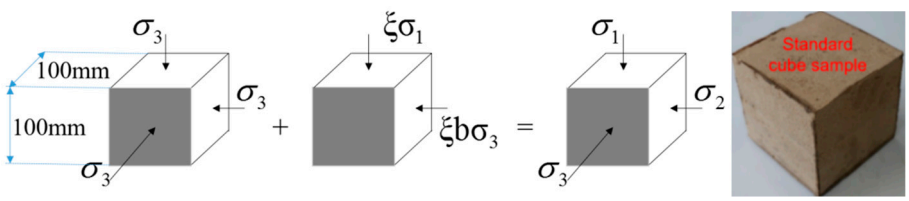


Figure 1. Test loading method.

Loading mode: For the test, we adopted a ZSZ-2000 microcomputer-controlled true triaxial frozen soil test platform. Figure 2 shows its loading device. The frozen soil triaxial test platform could realize independent sample loading in the three principal stress directions. The sample could be tested along different stress paths in the 3D stress space. The sample was loaded along the three principal stress directions using rigid plates. As shown in the three views in Figure 3, the F6 direction was the fixed end, which gave the reaction force in the F2 direction. Loading in the five directions, F1 to F5 was done independently by the servo cylinder through the force transmission rod. F3 and F5 were the loading directions of the first principal stress; F1 and F4 were the loading directions of the second principal stress; F2 and F6 were the third principal stress loading directions. Six steel plates were placed in a staggered overlap manner to realize the compression process of the sample. This test adopted a loading method with a constant principal stress ratio b in the control, where $b = (\sigma_2 - \sigma_3)/(\sigma_1 - \sigma_3)$. The parameter σ_3 was a constant. By shifting the term and taking the derivative of this formula, we find that $\xi(\sigma_2) = b\xi(\sigma_1)$, and ξ were the loading rate in the direction of the first principal stress, and $\xi = 25\text{N/s}$. The specific loading process of the test is shown in Figure 1. After the sample reached the required temperature for the test and stabilized for 30 min, a three-way synchronous pressure σ_3 was applied to place the specimen in a state of equal stress in the three directions. The specimen was then stabilized and consolidated until its deformation was unchanged. Different loading rates were subsequently set in the σ_1 and σ_2 directions. The ratio of the two loading rates was equal to b to realize the true triaxial test process while keeping b unchanged. The test failure threshold was when the deformation in the direction of the major principal strain reached 15 mm, that is $\varepsilon_1 = 15\%$, or when the test monitoring curve shows that the sample was evidently damaged, that is, when the strain in the first principal strain–first principal stress curve grew almost vertically, the corresponding strength was the failure strength.

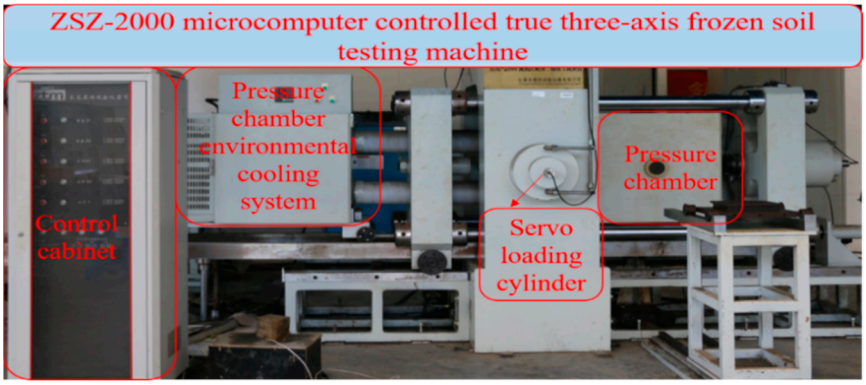


Figure 2. True triaxial test platform for frozen soil.

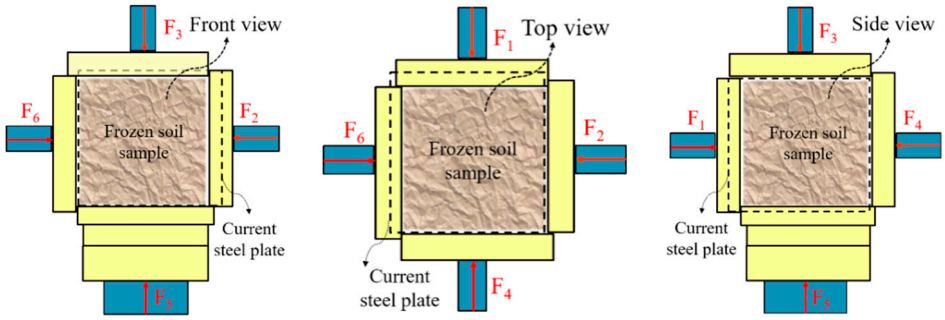


Figure 3. Three views of lapped rigid plates for frozen soil samples.

2.3. Test Results and Discussion

Considering that the test factors and loading environment of each sample of this true triaxial orthogonal test were different, there were many test curves; therefore, only some

test equivalent stress–strain curves were selected for the analysis, as shown in Figure 4, where q was the von Mises stress, see Equation (1). The first principal strain ε_1 was the sum of the strains in the F3 and F5 directions; the volume strain ε_v was the sum of the strains in directions F1 to F6, and the sign indicated that the pressure was positive.

$$q = \sqrt{\frac{1}{2}\left[(\sigma_1 - \sigma_2)^2 + (\sigma_2 - \sigma_3)^2 + (\sigma_3 - \sigma_1)^2\right]} \quad (1)$$

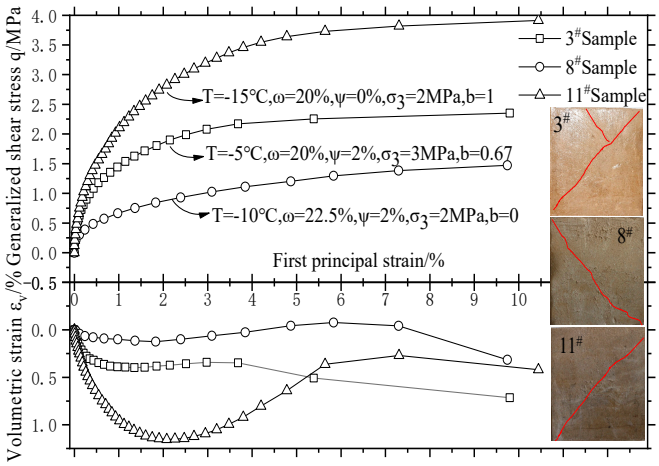


Figure 4. True triaxial stress–strain and volume deformation curves of frozen calcareous clay.

Figure 4 shows that the equivalent stress–strain relationship of the frozen calcareous clay was divided into three stages. The first was the linear elastic stage. Due to the high water content in the three selected samples, the samples were consolidated and frozen for a long duration. When the first principal strain was less than 0.5%, there was a certain instantaneous strength between the soil particles and cementation between the soil particles and ice crystals. Frozen soil samples exhibited good integrity and resistance to small deformations and rapid stress growth. The second was the plastic hardening stage. During this period, due to the increase in stress, the phenomenon of ice crystal pressure melting occurs. The soil and ice crystal particles, and pores reappeared in the frozen soil sample. The sample became denser, the bearing capacity was further improved, and plastic deformation from the first principal strain occurred, reaching approximately 5%. The third was the strain hardening failure stage. The occurrence of this stage depended on the test loading conditions. As mentioned above, a six-direction independent rigid loading mode was applied to control the load applied to the frozen soil samples. Frozen soil typically has certain residual stress after failure; if the frozen soil sample does not completely lose its bearing capacity or the test process was terminated, the force acting on the sample will continue to increase. As shown in Figure 4, the reason for the gradual growth in the deviator stress in the later stage was the rapid growth and expansion of the cracks in the sample under the action of the high stress applied (close to the ultimate bearing capacity). The samples expanded first and then shrank during the entire loading process. The expansion increased the gap between the rigid plates. When the specimen was placed between the rigid plates became incompressible, it overflowed from the gap between the plates, resulting in large deformation and unloading of the frozen soil specimens. This was also the reason for the evident shrinkage of the body.

Table 3 presents the results of the true triaxial orthogonal test conducted on the saline calcareous clay. The range analysis of the data listed in Table 3 was performed. Tables 4 and 5 list the analysis results. From a comparison of the R-values in Table 5, the primary and secondary order of influence affecting the peak strength σ_1 of frozen calcareous clay was as follows: pressure σ_3, water content ω, temperature T, Bishop parameter b, and salt content ψ. The primary and secondary order affecting σ_2 is shown in Table 6: the Bishop parameter b, confining pressure σ_3, water content ω, temperature T, and salt content

ψ. Comparing the value of L, factor C (that is, the salt content ψ) had a certain effect on the peak strength and second principal stress of frozen calcareous clay compared with the other four factors, but the degree of influence was weaker, and the four levels show a trend of first increasing and then decreasing. The Bishop parameter reflected the magnitude of the second principal stress. Therefore, the influence of this factor on the second principal stress was the most significant. This was self-evident; the sample was more compact, the existence of an external force increased the friction on the sliding surface, the cohesive force increased, and the peak strength increased. Existing research results show that [24,25] temperature was the main factor affecting the strength of frozen soil; this was because the moisture in the sample freezes in a low-temperature environment. The lower the temperature, the greater the volume percentage of the ice crystal cement. The lower the unfrozen water content, which increased the strength of the cementation between the soil particles, the higher the strength. However, the presence of salt changes the concentration of the aqueous solution in the sample, thereby changing its freezing temperature, and the water was difficult to freeze. Therefore, the greater the concentration of the salt solution, the greater the decrease in the peak intensity.

Table 3. Design and results of true triaxial orthogonal test conducted on saline calcareous clay [23].

Five-Factor and Four-Level ($L_{16}(4^5)$) Orthogonal Test on Saline Calcareous Clay							
Factor / Test Number	Temperature T/°C	Moisture Content ω/%	Salt Content ψ/%	Confining Pressure σ_3/MPa	Bishop Parameter b	Test Results	
						σ_{1max}/MPa	σ_{2max}/MPa
1	−5	15	0	1	0	3.789	1
2	−5	17.5	1	2	0.33	5.694	3.22
3	−5	20	2	3	0.67	5.35	4.58
4	−5	22.5	3	4	1	6.11	6.11
5	−10	15	1	3	1	10.209	10.209
6	−10	17.5	0	4	0.67	9.568	7.734
7	−10	20	3	1	0.33	3.064	1.683
8	−10	22.5	2	2	0	3.474	2
9	−15	15	2	4	0.33	10.396	6.102
10	−15	17.5	3	3	0	6.509	3
11	−15	20	0	2	1	5.914	5.914
12	−15	22.5	1	1	0.67	3.071	2.387
13	−20	15	3	2	0.67	7.94	5.981
14	−20	17.5	2	1	1	5.197	5.208
15	−20	20	1	4	0	8.411	4
16	−20	22.5	0	3	0.33	6.941	4.302

Table 4. Analysis of the degree of influence of various factors on the major principal stress σ_1 [23].

Factor Level		A	B	C	D	E	Optimal Level	Factor Priority
First principal stress σ_{1max}/MPa	L1	5.236	8.083	6.553	3.780	5.546	$A_4B_1C_2D_4E_4$	D > B > A > E > C
	L2	6.579	6.742	6.846	5.755	6.524		
	L3	6.473	5.685	6.104	7.252	6.482		
	L4	7.122	4.899	5.906	8.621	6.857		
	R	1.886	3.184	0.940	4.841	1.311		

Table 5. Analysis of the degree of influence of various factors on the intermediate principal stress σ_2 [23].

Factor Level		A	B	C	D	E	Optimal Level	Factor Priority
Second principal stress σ_{2max}/MPa	L1	3.728	5.823	4.737	2.570	2.500	$A_2B_1C_2D_4E_4$	E > D > B > A > C
	L2	5.406	4.790	4.954	4.279	3.827		
	L3	4.351	4.044	4.473	5.523	5.171		
	L4	4.873	3.700	4.194	5.987	6.860		
	R	1.678	2.123	0.760	3.417	4.360		

Table 6. Critical values of $F_\Omega(f_1,f_2)$ for F verification [26].

Significance Level Ω	0.1	0.05	0.01	0.005
$f_1 = 3, f_2 = 12$	2.606	3.490	5.953	7.230
$f_1 = 3, f_2 = 19$	2.397	3.13	5.010	\
$f_1 = 9, f_2 = 19$	1.984	2.42	3.523	\

To systematically study the relationship between the peak stress σ_1 and the intermediate principal stress σ_2 of frozen saline calcareous clay and the confining pressure σ_3, water content ω, temperature T, Bishop parameter b, and salt content ψ, according to the dimension analysis theory, an exponential function was used to compare the test data in Table 4. The calculation formula could be obtained by fitting in Origin as follows:

$$\sigma_1 = 86.6208T^{0.1975} \cdot \omega^{-1.23085} \cdot \psi^{-0.00776} \cdot \sigma_3^{0.59654} \cdot b^{0.02066}, R^2 = 0.966 \quad (2)$$

To more intuitively reflect the significant effects of the confining pressure and water content on the peak stress and the second principal stress in the range analysis, the confining pressure σ_3 and water content ω were drawn for a temperature $T = -10$ °C and salt content $\psi = 1\%$. Figures 5 and 6 show the 3D trend charts of the peak stress σ_1 and second principal stress σ_2 under different b values, respectively.

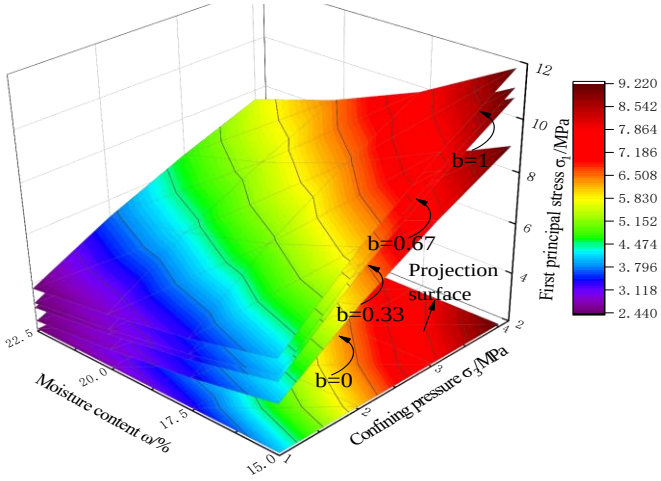


Figure 5. Three-dimensional trend chart of water content, confining pressure, and high principal stress under different b values [23].

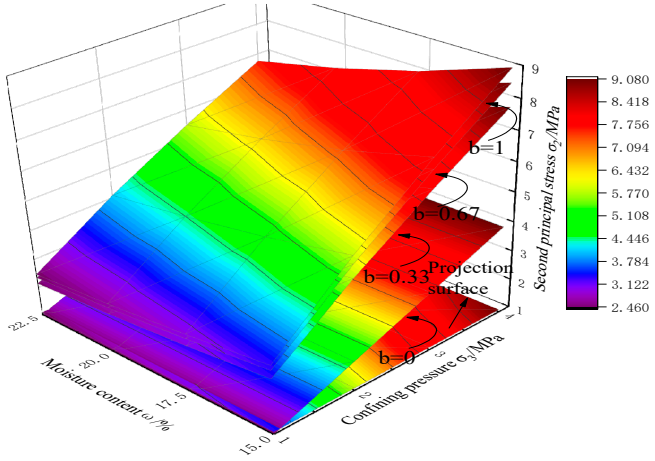


Figure 6. Three-dimensional trend chart of water content, confining pressure, and intermediate principal stress under different b values [23].

Figure 5 shows that as the value of b increases, the slope of the curved surface becomes steeper, indicating that an increase in b directly increased the stress in the σ_2 direction, the average principal stress increased, and the frozen soil was compacted. Although the second principal stress also increased, it accelerated the melting effect of ice crystals in the frozen soil and increased the restraint and occlusion of soil particles. Therefore, the strength significantly increased when $b = 0$ or $b \neq 0$, while the peak stress between $b = 0.33$ and 1 gradually decreased. This was because although the stress in the σ_2 direction increased, the occlusion between the soil particles was increased to a certain extent, and the strength was increased; however, the σ_3 direction constraint remained unchanged. The principal stress σ_1 significantly increased, and the strength of the sample decreased as the moisture content increased; the change in the moisture content cannot significantly affect the first principal stress σ_1. For example, when the confining pressure was 1 MPa, the first principal stress was 4.895 MPa for 15% water content, and the first principal stress was 2.972 MPa for 22.5% water content, which was reduced by 1.923 MPa, and the rate of change was 39.3%. The confining pressure had a significant influence on the first principal stress σ_1. For example, when the water content was 15%, the first principal stress with a confining pressure of 1 MPa was 4.895 MPa, and the first principal stress with a confining pressure of 4 MPa was as high as 11.193 MPa, which was an increase of 6.298 MPa, and the rate of change was 56.3%.

The 3D trend chart of σ_2 under different b values, shown in Figure 6, was the same as that of the peak stress σ_1 because σ_2 and σ_1 were dependent on each other. When the stress in the σ_1 direction reached the peak, the sample was broken, and there was no room for growth in σ_2. As the confining pressure increased, the sample was sufficiently dense, and it was difficult for dilatancy to occur. The restraint and compaction effect of σ_2 became insignificant; therefore, the distance between the curved surfaces became smaller as the value of b increased; the water content increased under freezing conditions. The most intuitive effect of the enhancement in the peak stress of the soil was the volume content of the ice crystals in the frozen soil and the cementation of the ice crystals on the soil particles. However, the increase in the confining pressure also caused compression and melting and weakened the contribution of the increase in the water content to the increase in the peak stress. Therefore, the confining pressure was the main significant factor for the increase in the peak stress and the second principal stress, whereas, for the stress in the σ_2 direction, the b value was the most significant factor. For example, when the confining pressure was 4 MPa, the Bishop parameter b increased from 0 to 1, and the corresponding second principal stress increased from 4 to 9.128 MPa, which was an evident increase.

3. Levels of Analysis

The range analysis method was conducted to obtain the order of priority among the influencing factors without considering the interaction of the various factors. However, it was not possible to obtain the influence of the factors and their levels on the test results' influence weight. Therefore, the analytic hierarchy process was introduced to explore the weights of the above five factors on the strength of the frozen calcareous clay.

3.1. Hierarchical Analysis Theory

Similar to Table 2, considering its more general situation, we supposed that there were k influencing factors, namely $A^{(1)}$, $A^{(2)}$, ... , $A^{(k)}$, and the number of levels of each factor was n_1, n_2, ... , n_k. As shown in Figure 7, the AHP model of the orthogonal experiment had a three-layer structure comprising the index, factor, and level layers.

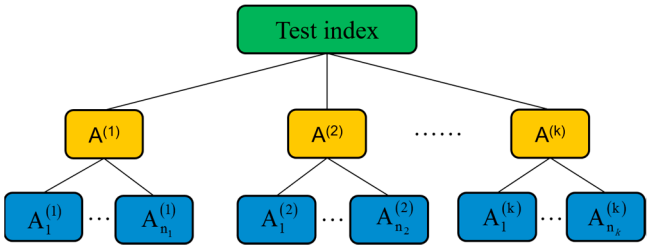


Figure 7. Orthogonal test AHP model.

Therefore, the sum of the test data under the j-th level of the defined factors were called the influence effect of the j-th level of the factor on the test, where $i = 1, 2 \ldots, k$; $j = 1, 2 \ldots, n_k$. If the value of the inspection test index was high, let $M_{ij} = K_{ij}$; otherwise, let $M_{ij} = 1/K_{ij}$. Among them, the effect matrix of the horizontal layer on the experiment is shown in Equation (3), and S is expressed in Equation (4).

$$A = \begin{pmatrix} M_{11} & 0 & \cdots & 0 \\ M_{21} & 0 & \cdots & 0 \\ \cdots & \cdots & \cdots & \cdots \\ M_{n_1 1} & 0 & \cdots & 0 \\ 0 & M_{12} & \cdots & 0 \\ 0 & M_{22} & \cdots & 0 \\ \cdots & \cdots & \cdots & \cdots \\ 0 & M_{n_2 2} & \cdots & 0 \\ \cdots & \cdots & \cdots & \cdots \\ 0 & 0 & \cdots & M_{1k} \\ 0 & 0 & \cdots & M_{2k} \\ \cdots & \cdots & \cdots & \cdots \\ 0 & 0 & \cdots & M_{n_k k} \end{pmatrix} \tag{3}$$

$$S = \begin{pmatrix} 1/t_1 & 0 & \cdots & 0 \\ 0 & 1/t_2 & \cdots & 0 \\ \cdots & \cdots & \cdots & \cdots \\ 0 & 0 & \cdots & 1/t_k \end{pmatrix} \tag{4}$$

where $t_j = \sum_{i=1}^{n_j} M_{ij} \quad (j = 1, 2, \cdots, k)$.

Therefore, matrix A right multiplied by matrix S was the normalization process of each column of matrix A, and matrix AS was called the level standard influence effect matrix. The range of the factors was R_i ($i = 1, 2, \ldots, m$), which was called the influence of factors on the experiment. The weight matrix of the influence of factors on the experiment is expressed in Equation (5):

$$C = \left(\frac{R_1}{\sum_{i=1}^{m} R_i} \quad \frac{R_2}{\sum_{i=1}^{m} R_i} \quad \cdots \quad \frac{R_m}{\sum_{i=1}^{m} R_i} \right) \tag{5}$$

Finally, the influence weight of each factor level on the index $\varpi = ASC^T$ was obtained by the analytic hierarchy process. ϖ was $(n^{1+}\ n^{2+} \ldots\ n^{k+}) \times 1$ vector, which indicated the influence of each level of the factor on the experiment.

3.2. Discussion on the AHP Result

The above method yields the following:

$$C = \begin{pmatrix} 0.155 & 0.262 & 0.077 & 0.398 & 0.108 \end{pmatrix} \tag{6}$$

$$S = \begin{pmatrix} 0.039 & 0 & \cdots & 0 \\ 0 & 0.039 & \cdots & 0 \\ \cdots & \cdots & \cdots & \cdots \\ 0 & 0 & \cdots & 0.039 \end{pmatrix}_{5\times5} \tag{7}$$

$$A = \begin{pmatrix} 5.236 & 0 & 0 & 0 & 0 \\ 6.579 & 0 & 0 & 0 & 0 \\ 6.473 & 0 & 0 & 0 & 0 \\ 7.122 & 0 & 0 & 0 & 0 \\ 0 & 8.084 & 0 & 0 & 0 \\ 0 & 6.742 & 0 & 0 & 0 \\ 0 & 5.685 & 0 & 0 & 0 \\ 0 & 4.899 & 0 & 0 & 0 \\ 0 & 0 & 6.533 & 0 & 0 \\ 0 & 0 & 6.846 & 0 & 0 \\ 0 & 00 & 6.104 & 0 & 0 \\ 0 & 0 & 5.906 & 0 & 0 \\ 0 & 0 & 0 & 3.780 & 0 \\ 0 & 0 & 0 & 5.756 & 0 \\ 0 & 0 & 0 & 7.252 & 0 \\ 0 & 0 & 0 & 8.621 & 0 \\ 0 & 0 & 0 & 0 & 5.546 \\ 0 & 0 & 0 & 0 & 6.524 \\ 0 & 0 & 0 & 0 & 6.482 \\ 0 & 0 & 0 & 0 & 6.856 \end{pmatrix} \tag{8}$$

Therefore, the degree of influence of the various factors on the peak intensity σ_1 was as follows:

$$\varpi_1 = ASC^T = \begin{pmatrix} 5.236 & 0 & 0 & 0 & 0 \\ 6.579 & 0 & 0 & 0 & 0 \\ 6.473 & 0 & 0 & 0 & 0 \\ 7.122 & 0 & 0 & 0 & 0 \\ 0 & 8.084 & 0 & 0 & 0 \\ 0 & 6.742 & 0 & 0 & 0 \\ 0 & 5.685 & 0 & 0 & 0 \\ 0 & 4.899 & 0 & 0 & 0 \\ 0 & 0 & 6.533 & 0 & 0 \\ 0 & 0 & 6.846 & 0 & 0 \\ 0 & 00 & 6.104 & 0 & 0 \\ 0 & 0 & 5.906 & 0 & 0 \\ 0 & 0 & 0 & 3.780 & 0 \\ 0 & 0 & 0 & 5.756 & 0 \\ 0 & 0 & 0 & 7.252 & 0 \\ 0 & 0 & 0 & 8.621 & 0 \\ 0 & 0 & 0 & 0 & 5.546 \\ 0 & 0 & 0 & 0 & 6.524 \\ 0 & 0 & 0 & 0 & 6.482 \\ 0 & 0 & 0 & 0 & 6.856 \end{pmatrix} \begin{pmatrix} 0.039 & 0 & \cdots & 0 \\ 0 & 0.039 & \cdots & 0 \\ \cdots & \cdots & \cdots & \cdots \\ 0 & 0 & \cdots & 0.039 \end{pmatrix}_{5\times5} \begin{pmatrix} 0.155 \\ 0.262 \\ 0.077 \\ 0.389 \\ 0.108 \end{pmatrix} = \begin{pmatrix} 0.0317 \\ 0.0389 \\ 0.0391 \\ 0.0431 \\ 0.0826 \\ 0.0689 \\ 0.0581 \\ 0.0501 \\ 0.0197 \\ 0.0206 \\ 0.0183 \\ 0.0177 \\ 0.0587 \\ 0.0893 \\ 0.1126 \\ 0.1338 \\ 0.0234 \\ 0.0275 \\ 0.0289 \\ 0.0273 \end{pmatrix} \tag{9}$$

$$\varpi_1 = ASC^T = \begin{pmatrix} 3.728 & 0 & 0 & 0 & 0 \\ 5.406 & 0 & 0 & 0 & 0 \\ 4.351 & 0 & 0 & 0 & 0 \\ 4.873 & 0 & 0 & 0 & 0 \\ 0 & 5.823 & 0 & 0 & 0 \\ 0 & 4.790 & 0 & 0 & 0 \\ 0 & 4.044 & 0 & 0 & 0 \\ 0 & 3.700 & 0 & 0 & 0 \\ 0 & 0 & 4.737 & 0 & 0 \\ 0 & 0 & 4.954 & 0 & 0 \\ 0 & 00 & 4.473 & 0 & 0 \\ 0 & 0 & 4.194 & 0 & 0 \\ 0 & 0 & 0 & 2.570 & 0 \\ 0 & 0 & 0 & 4.279 & 0 \\ 0 & 0 & 0 & 5.523 & 0 \\ 0 & 0 & 0 & 4.194 & 0 \\ 0 & 0 & 0 & 0 & 2.500 \\ 0 & 0 & 0 & 0 & 3.827 \\ 0 & 0 & 0 & 0 & 5.171 \\ 0 & 0 & 0 & 0 & 6.860 \end{pmatrix} \begin{pmatrix} 0.054 & 0 & \cdots & 0 \\ 0 & 0.054 & \cdots & 0 \\ \cdots & \cdots & \cdots & \cdots \\ 0 & 0 & \cdots & 0.054 \end{pmatrix}_{5\times5} \begin{pmatrix} 0.136 \\ 0.172 \\ 0.062 \\ 0.277 \\ 0.354 \end{pmatrix} = \begin{pmatrix} 0.0274 \\ 0.0397 \\ 0.0320 \\ 0.0358 \\ 0.0541 \\ 0.0445 \\ 0.0376 \\ 0.0344 \\ 0.0159 \\ 0.0166 \\ 0.0150 \\ 0.0140 \\ 0.0384 \\ 0.0640 \\ 0.0826 \\ 0.0896 \\ 0.4460 \\ 0.6828 \\ 0.9226 \\ 1.2239 \end{pmatrix} \quad (10)$$

From the calculation result obtained using Equation (9) without considering the interaction, the four levels of each factor have the highest influence weight on the peak stress σ_1: factor A was A_4 = 0.0431; factor B was B_1 = 0.0826; factor C was C_2 = 0.0206; factor D was D_4 = 0.1338; and factor E was E_4 = 0.0289. Thus, the optimal level of the experiment was $A_4B_1C_2D_4E_4$, and the primary and secondary order of influence of each factor was determined by the sum of the weights at each level of the five factors. The order of the primary and secondary influence of each factor was D > B > A > E > C. Similarly, the degree of influence of each factor on the intermediate principal stress σ_2 was obtained. As expressed in Equation (10), the weights with the highest influence were A_2 = 0.397; B_1 = 0.0541; C_2 = 0.0166; D_4 = 0.0896; and E_4 = 1.2239. The optimal level of σ_2 was E > D > B > A > C. Both these results were consistent with the range analysis results. Moreover, the influence weight of each level of the factor on the peak intensity was obtained through the analytic hierarchy process.

4. Significance and Interaction Analysis

4.1. Significance Analysis Method

The magnitude of the variation was characterized by the sum of the squares of the variation, which was defined as:

$$S_i = \sum_{i=1}^{n} (x_i - \widetilde{x})^2 \quad (11)$$

where, $\widetilde{x} = \frac{1}{n}\sum_{i=1}^{n} x_i$.

The estimated value of the deviation SS_i was expressed as:

$$SS_i = Q_i \Big/ f_i \quad (12)$$

where f was the degree of freedom, and $f_T = N - 1$, N was the total number of trials, $f_i = k - 1$, k was the level of factor i, $f_e = f_T - f_i$.

Based on the above deviation definition method, the calculation process of the significance level of the five-factor four-level orthogonal test reported in this paper was as follows:

The sum of the squared deviations S_T was:

$$S_T = \sum_{i=1}^{16} x_i^2 - \frac{1}{16}\left(\sum_{i=1}^{16} x_i\right)^2 \tag{13}$$

Let $\eta = \frac{1}{16}\left(\sum_{i=1}^{16} x_i\right)^2$. From the data listed in Table 3, we obtained η= 645.63; then, the sum of the squared deviations of each factor $S_A, S_B, \ldots, S_E$ was expressed as:

$$\begin{aligned} S_A &= \tfrac{1}{4}\sum_{i=1}^{4} T_{Ai}^2 - \tfrac{1}{16}\left(\sum_{i=1}^{16} x_i\right)^2 \\ S_B &= \tfrac{1}{4}\sum_{i=1}^{4} T_{Bi}^2 - \tfrac{1}{16}\left(\sum_{i=1}^{16} x_i\right)^2 \\ &\cdots\cdots \\ S_E &= \tfrac{1}{4}\sum_{i=1}^{4} T_{Ei}^2 - \tfrac{1}{16}\left(\sum_{i=1}^{16} x_i\right)^2 \end{aligned} \tag{14}$$

In the formula: $T_{Ai}, T_{Bi}, \cdots, T_{Ei}$ were the sum of the test values of each factor at a certain level, e.g., T_{Ai} was the sum of the four groups of test values at the level of factor 1.

The sum of squares of the error effect deviation S_e was:

$$S_e = S_T - (S_A + S_B + \cdots + S_E) \tag{15}$$

The sum of the squared deviations of the error effect reflected the fluctuation value of the test error in this set of data. From Equations (13)–(15), the sum of the squared deviations corresponding to each factor was obtained. For example, the calculation process of S_A was:

$$\begin{aligned} T_{A1} &= (3.789 + 5.694 + 5.35 + 6.11) = 20.943 \\ S_A &= (20.9432 + 26.3152 + 25.892 + 28.4892)/4 - 645.63 = 7.621 \end{aligned} \tag{16}$$

Table 7 presents the rest of the calculation results. Referring to the corresponding degrees of freedom of the factors according to Equation (12), the estimated value of the deviation SS_i of each factor was determined.

Table 7. Significance test on influencing factors of peak intensity σ_1.

Factor	Sum of Squares	Degrees of Freedom	F Ratio	Significance
A	7.621	3	3.494	III
B	22.826	3	10.466	II
C	2.181	3	1.000	V
D	51.719	3	23.713	I
E	3.808	3	1.746	IV
Error	2.18	12	0.01	\
Sum	88.152	15	\	\

Considering the ratio of deviation estimates:

$$F_i = \frac{SS_i}{SS_e} = \frac{S_i/f_i}{S_e/f_e} \tag{17}$$

For a given significance level Ω, if

$$F_i \geq F_\Omega(f_i, \quad f_e) \tag{18}$$

The influence of factor i on the test index was significant; otherwise, it was not significant.

4.2. Significance Analysis without Considering Interaction

The test data listed in Table 3 were calculated and tested using the above calculation method, and the critical values of the F test listed in Table 6 were compared. Table 7 lists the test results.

The results of the significance study of the peak stress σ_1 showed that under complex stress conditions (under true triaxial conditions), the confining pressure and water content had significant effects on the strength, and the temperature effect was significant when $\Omega > 0.05$. The influences of the salt content and b value on the intensity were not very significant. The order of significance of each factor was consistent with the results of the range analysis method and analytic hierarchy process.

4.3. Significance Analysis Considering Interaction

In the real state, the influence of frozen soil strength was not the result of single factors that were independently affected and then simply superimposed. The interactive influence of various factors could not be ignored. For example, the water content was the factor determining the volumetric ice content of frozen soil. However, an increase in the salt content reduced the freezing temperature of the water in the soil, making it difficult to freeze, and the volumetric ice content naturally decreased, thereby reducing the strength. At the same time, the application of a confining pressure caused the compression–thaw effect in the frozen soil, and the ice crystal cementation and melting affected the intensity. There were complex interactions between the various factors affecting the intensity. The above analysis results that did not consider the interaction between the factors could only be qualitatively analyzed to a certain extent. Hence, it was necessary to make the following significance analysis considering these interactions.

According to the basic idea of the orthogonal experiment design, the $L_{32}(4^9)$ orthogonal experiment table was used to design the experiment. The orthogonal experiment table head design was implemented in strict accordance with the experimental procedures. Due to many factors, the table head was too large, and the table head design is not presented herein. This study only considered the interaction between factors A, B, and C. Some of the 32 groups of effective tests were consistent with the test conditions listed in Table 3, and the test results could be used. Most of the remaining test results were calculated from Equation (2). The data obtained were analyzed for significance using the method described in Section 4.1. Table 8 presents the results.

Table 8. Significance test of factors affecting the peak intensity σ_1 when the interaction was considered.

Factor	Sum of Squares	Degrees of Freedom	F Ratio	Significance
A	5.286	3	2.259	V
B	46.950	3	20.064	II
A × B	8.259	9	3.529	IV
C	2.340	3	1.000	VIII
A × C	4.606	9	1.968	VI
B × C	2.547	9	1.088	VII
D	81.744	3	34.933	I
E	18.564	3	7.933	III
Error	2.34	19	0.01	\
Sum	173.296	31	\	\

The test results showed that for the significance levels listed in Table 6, the effects of the confining pressure, water content, and intermediate principal stress coefficient b on the peak stress were all significant; the interactions A × B, A × C, and B × C had different degrees of influence on σ_1, and the significance of the three interactions exceeded the degree of influence of the salt content. When $\Omega > 0.01$, the influence of A × B on the equivalent

stress was significant, and its influence even exceeded that of the temperature. From the results listed in Table 8, we concluded that the order of significance of the influence of various factors on the peak stress was as follows: confining pressure D, water content B, intermediate principal stress coefficient b, interaction A × B, temperature A, interaction A × C, interaction B × C, and salt content C. Hence, when studying the strength of frozen soil, it was necessary to comprehensively consider the various factors and their interactions to more accurately characterize the mechanical behavior of frozen soil.

5. Conclusions

In this study, a true triaxial orthogonal test was conducted on frozen calcareous clay to explore its strength change characteristics under the influence of multiple factors, including the degree of influence of each factor. The following conclusions were drawn from the results:

(1) The characteristics of the stress–strain curve of frozen calcareous clay could be divided into three stages: the strain was within 0.5%, showing linear elasticity, and under the effect of pressure, the ice crystals, and their cements were damaged or compressed, and they shrink; at approximately 5%, they showed plastic hardening. The soil particles and ice crystals in the frozen soil recombined and became denser, resulting in irreversible deformation. With the compression process, cracks bred and expanded. The failure stage was manifested as strain hardening due to the test loading conditions. As the deformation increased, the stress also slightly increased. In this stage, the soil sample was squeezed out, and the volume deformation could not represent its true change.

(2) Through analytic hierarchy process, the peak stress σ_1 of each factor under four levels was quantitatively calculated, and the maximum value of influence weight of σ_1 was $A_4 = 0.0431$; $B_1 = 0.0826$; $C_2 = 0.0206$; and $D_4 = 0.1338$; $E_4 = 0.0289$, the maximum and minimum weight was 0.1338 and 0.0197, respectively, and the optimal level was $A_4B_1C_2D_4E_4$. By comparing the sum of the weights of the four levels of each factor, the order of primary and secondary influence consistent with the range method was obtained, which was D > B > A > E > C. Similarly, the maximum and minimum weight of σ_2 was 1.2239 and 0.014, respectively, and the order of σ_2 was E > D >B > A > C.

(3) When the interaction was not considered under true triaxial conditions, the effects of the confining pressure and water content on the strength were always significant. The temperature effect was significant only when the significance level $\Omega > 0.05$. The salinity and b value had a significant effect on the strength. The impact was not significant, and the ranking of the significance of each factor was consistent with the results of the range analysis method and the analytic hierarchy process. When considering the interaction, the interaction factors had different effects on the intensity. When $\Omega > 0.01$, A × B was equivalent, and the effect of stress was significant, even exceeding that of the temperature. When studying the strength of frozen soil, it was necessary to comprehensively consider the various factors and the interaction between them, to more accurately characterize the mechanical behavior of frozen soil.

Author Contributions: Conceptualization, Z.W. and C.-X.R.; methodology, Z.W. and C.-X.R.; software, Z.W. and Y.C.; validation, C.-X.R., Z.W. and Y.C.; formal analysis, Z.W.; investigation, Q.Y.; resources, Z.W.; data curation, W.L.; writing—original draft preparation, Z.W.; writing—review and editing, Z.W. and W.L.; visualization, Q.Y.; supervision, C.-X.R.; project administration, Z.W.; funding acquisition, C.-X.R. All authors have read and agreed to the published version of the manuscript.

Funding: This research was funded by the National Natural Science Foundation of China (grant numbers 51878005 and 51374010); and the Engineering Research Center of the Ministry of Education of Anhui University of Science and Technology in 2020 (grant number: JYBGCZX2020209).

Institutional Review Board Statement: Not applicable.

Informed Consent Statement: Not applicable.

Data Availability Statement: Not applicable.

Acknowledgments: This work was supported by Grants-in-Aid for scientific research from the National Natural Science Foundation of China (51878005, 51374010), Engineering Research Center of the Ministry of Education of Anhui University of Science and Technology in 2020 (JYBGCZX2020209).

Conflicts of Interest: The authors declare no conflict of interest.

References

1. Lu, L.N.; Fan, H.H.; Chen, H.; Ma, D.L.; Wang, Z.N.; He, Z.Q. Experimental study on influencing factors of uniaxial tensile strength of dispersive soil. *Chin. J. Geotech. Eng.* **2014**, *36*, 1160–1166.
2. Lv, H.B.; Zeng, Z.T.; Ge, R.L.; Zhao, Y.L. Experimental study on tensile strength of swelling and shrinking soil. *Rock Soil Mech.* **2013**, *34*, 615–620, 638.
3. Liu, B.; Sun, Y.D.; Yuan, Y.F.; Liu, X.C.; Bai, X.T.; Fang, T.J. Strength characteristics and strengthening mechanism of frozen sandstone with different water content. *J. China Univ. Min. Technol.* **2020**, *49*, 1085–1093, 1127.
4. Chen, L.H. Correlation and non-correlation regression statistics of probability characteristics of shear strength. *J. Geotech. Eng.* **2013**, *35*, 1397–1402.
5. Chen, C.L.; Zhang, H.M. Some Problems in Triaxial Test of Saturated Sand. *Chin. J. Geotech. Eng.* **2000**, *22*, 659–663.
6. Gen, H.H.; Wu, J.Y.; Shan, R.L.; Huang, B. Study on the Suction Contribution Form of Unsaturated Soil Strength. *Chin. J. Geotech. Eng.* **2012**, *34*, 1598–1603.
7. Li, K.Q.; Li, D.Q.; Liu, Y. Meso-scale investigations on the effective thermal conductivity of multi-phase materials using the finite element method. *Int. J. Heat Mass Transf.* **2020**, *151*, 119383. [CrossRef]
8. Li, K.Q.; Miao, Z.; Li, D.Q.; Liu, Y. Effect of mesoscale internal structure on effective thermal conductivity of anisotropic geomaterials. *Acta Geotech.* **2022**, *17*, 3553–3566. [CrossRef]
9. Cai, Z.Y.; Wu, Z.Q.; Huang, Y.H.; Cao, Y.Y.; Wei, Y.B. Geotechnical Engineering Department, Influence of water and salt contents on strength of frozen soils. *Chin. J. Geotech. Eng.* **2014**, *36*, 1580–1586.
10. Niu, Y.Q.; Lai, Y.M.; Wang, X.; Liao, M.K.; Gao, J. Study on the influence of initial moisture content on the deformation and strength of frozen silty clay. *Rock Soil Mech.* **2016**, *37*, 499–506.
11. Lai, Y.M.; Zhang, Y.; Zhang, S.J.; Jin, L.; Chang, X.X. The influence of supersaturated water content and temperature on the strength of frozen sand. *Rock Soil Mech.* **2009**, *30*, 3665–3670.
12. Du, H.M.; Ma, W.; Zhang, S.; Zhou, Z.W. Study on the influence characteristics of confining pressure and water content on the failure strain energy density of frozen sand. *Rock Soil Mech.* **2017**, *38*, 1943–1950.
13. Xiao, H. The relationship between the uniaxial compressive strength of artificial frozen soil and temperature and water content. *Geotech. Eng.* **2008**, *11*, 62–63, 76.
14. Yin, Z.Z.; Chen, Y.L.; Wang, P. Uniaxial unconfined compressive strength test on artificially frozen clay in Shanghai. *Rock Soil Mech.* **2012**, *33*, 788–792.
15. Sun, L.Q.; Lu, J.X.; Li, H.; Yan, S.W.; Jia, X.; Han, S.Z. Experimental study on the influence of water content and salt content on the strength characteristics of artificial frozen soil. *Chin. J. Geotech. Eng.* **2015**, *37*, 27–31.
16. Ge, X.X.; Yang, Z.H.; Still, B. Mechanical properties of naturally frozen silty soil for seismic design of pile foundations.10th International Symposium on Cold Regions Development. *Reston: Am. Soc. Civ. Eng.* **2013**, *32*, 215–227.
17. Ma, X.J.; Zhang, J.M.; Chang, X.X.; Zheng, B.; Zhang, M.Y. Experimental research on strength of warm and ice-rich frozen clays. *Rock Soil Mech.* **2008**, *229*, 2498–2502.
18. Dai, J.Q.; Su, Z.J.; Zhao, M.C.; Xiang, Y.H. Study on true triaxial test and strength characteristics of silty clay. *Rock Soil Mech.* **2016**, *37*, 2534–2540, 2546.
19. Chen, C.L.; Shao, S.J.; Zhang, Z. Study on true triaxial test of artificially prepared structural loess. *Rock Soil Mech.* **2013**, *34*, 2231–2237.
20. Ma, S.L.; Yao, Z.M.; Liu, S.; Pan, X. Damage Constitutive Model of Frozen Sand under the Influence of Intermediate Principal Stress Coefficient. *Coal Field Geol. Explor.* **2020**, *48*, 130–136.
21. Zhang, M.; Xu, C.S.; Du, X.L.; Wang, G.S.; Lu, D.C. Study on true triaxial test of the influence of intermediate principal stress coefficient and stress path on the shear characteristics of sand. *J. Hydraul. Eng.* **2015**, *46*, 1072–1079.
22. Wang, Z.; Rong, C.; Du, M.; Ma, M.; Liu, X. The development law of freezing temperature field of calcareous clay layer. *Math. Probl. Eng.* **2020**, *2022*, 3902054. [CrossRef]
23. Cao, Y.; Rong, C.; Wang, Z.; Shi, X.; Wang, B.; Long, W. Experimental Study on True Triaxial Mechanical Properties of Frozen Calcareous Clay under the Influence of Multiple Factors. *Crystals* **2022**, *12*, 328. [CrossRef]
24. Bai, R.; Xu, X.; Hua, S.; Wang, J. Significant analysis of the influence factors on strength of frozen soil base on multivariable linear regression model. *J. Glaciol. Geocryol.* **2019**, *41*, 416–423.
25. Chou, Y.L.; Jiang, X.G.; He, B.B.; Sheng, Y. Experimental study on mechanical properties of frozen loess based on structure. *J. Glaciol. Geocryol.* **2014**, *36*, 913–921.
26. Teng, S.Z.; Feng, J.H. *Mathematical Statistics*; Dalian University of Technology Press: Dalian, China, 2005.